The EMBO Journal vol.13 no.8 pp.1806 – 1816, 1994

The mouse *lethal nonagouti* (a^x) mutation deletes the *S-adenosylhomocysteine hydrolase* (*Ahcy*) gene

Miles W.Miller, David M.J.Duhl, Ben M.Winkes, Francisco Arredondo-Vega[1], Paul J.Saxon[2,3], George L.Wolff[4], Charles J.Epstein[2], Michael S.Hershfield[1] and Gregory S.Barsh[5]

Department of Pediatrics and Howard Hughes Medical Institute, Stanford University School of Medicine, Stanford, CA 94305-5428, [1]Departments of Medicine and Biochemistry, Duke University Medical Center, Durham, NC 27710-0001, [2]Department of Pediatrics, University of California, San Francisco, CA 94143-0748 and [4]National Center for Toxicological Research, Food and Drug Administration, US Department of Health and Human Services, Jefferson, AR 72079-9590, USA

[3]Present address: Department of Laboratory Medicine, Sutter Memorial Hospital, Sacramento, CA 95819, USA

[5]Corresponding author

Communicated by R.Nusse

The *lethal nonagouti* (a^x) mutation is a hypomorphic allele of the *agouti* coat color locus which, when homozygous, also leads to embryonic death around the time of implantation. To understand the molecular basis of these phenotypes, we identified and cloned a deletion breakpoint junction present in the a^x chromosome. Long range restriction mapping demonstrated a simple deletion of ~100 kb, which does not affect *agouti* coding sequences, but begins only 4 kb 3′ of the last exon, and thus may affect coat color by removing an *agouti* 3′ enhancer. The *Ahcy* gene, which codes for the enzyme *S*-adenosylhomocysteine hydrolase (SAHase), is contained within a 20 kb region within the a^x deletion. SAHase RNA and protein were detectable in early blastocysts and in embryonic stem cells, respectively, and analysis of embryos derived from an $a^x/a \times a^x/a$ embryo intercross indicated that a^x/a embryos die between the late blastocyst and early implantation stages. Treatment of cultured embryos with an SAHase inhibitor, 3-deaza-aristeromycin, or with metabolites that can result in elevated levels of cellular SAH, resulted in an inhibition of inner cell mass development, suggesting that loss of SAHase activity in a^x/a^x embryos is sufficient to explain their death around the time of implantation.

Key words: *S*-adenosylhomocysteine hydrolase/*agouti*/methyltransferase/mouse development

Introduction

Valuable insights into mammalian development have been gained by molecular characterization of mouse embryonic lethal mutations (reviewed in Magnuson, 1986). Some recessive lethal mutations that have been pursued in this way were caused by insertion of a provirus or transgene, but many others were the product of large-scale mutagenesis experiments or arose spontaneously during the derivation of inbred strains (Russell, 1951; Schnieke *et al.*, 1983; Costantini *et al.*, 1989; Niswander *et al.*, 1989; Herrmann *et al.*, 1990; Friedrich and Soriano, 1991; Lee *et al.*, 1992).

Among the oldest known and best-characterized mouse embryonic lethal mutations are the *lethal yellow* (A^y) and *lethal nonagouti* (a^x) alleles, which define two of at least three different embryonic lethal complementation groups in the *agouti* locus, but affect agouti coat color in opposite ways (Cuènot, 1908; Robertson, 1942; Russell *et al.*, 1963; Papaioannou and Mardon, 1983; Lyon *et al.*, 1985; reviewed in Siracusa, 1991). The a^x allele is hypomorphic with regard to coat color, compared with mice homozygous for a complete loss-of-function *agouti* allele such as *extreme nonagouti* (a^e), which are wholly black, a^x/a^e mice have a lighter ventrum and flanks (Barsh and Epstein, 1989b). In contrast, the A^y allele is hypermorphic with regard to coat color; A^y/a^e mice are completely yellow.

Histologic studies of embryos derived from $A^y/- \times A^y/-$ and $a^x/- \times a^x/-$ intercrosses suggest that, in both cases, homozygous mutant embryos die around the time of implantation (Robertson, 1942; Eaton and Green, 1962; Pedersen, 1974; Cizadlo and Granholm, 1978; Papaioannou and Mardon, 1983). The exact times and causes of death are not clear, in part because it has not been possible until recently to determine the genotype of individual embryos derived from such intercrosses. Other *agouti* alleles which are not recessive lethals exhibit similar or identical coat color phenotypes to A^y and a^x (Silvers, 1979; Wolff *et al.*, 1986; Green, 1989), therefore embryonic lethality associated with these mutations may be due to altered expression of one or more genes that are closely linked to, but distinct from the *agouti* coat color gene.

Some insight into these questions has come from the recent cloning and molecular characterization of *agouti*, which appears to code for a paracrine signaling molecule expressed by non-pigment cells within hair follicles (Bultman *et al.*, 1992; Miller *et al.*, 1993). *Agouti* is also expressed normally during embryonic development (Vrieling *et al.*, 1994), and, when ubiquitously expressed as in the A^y or A^{vy} mutations, can affect regulation of body size and tumor susceptibility (reviewed in Yen *et al.*, 1994). To investigate a possible relationship between the *agouti* coat color gene and embryonic development, and to understand better what kinds of molecular and physiologic defects are responsible for peri-implantation lethality of A^y/A^y and a^x/a^x embryos, we have attempted to determine the molecular lesions responsible for these mutations. Here were report that the a^x mutation is caused by a 100 kb deletion of DNA close to but not within the *agouti* gene, which suggests that *cis*-acting elements required for normal *agouti* expression may lie in its 3′ flanking sequence. Notably, the deletion completely removes a gene adjacent to *agouti*, *Ahcy*, that encodes the enzyme *S*-adenosylhomocysteine hydrolase (SAHase), which plays a key role in the regulation of *S*-adenosylmethionine (SAM)-

dependent transmethylation and methylation-dependent cellular processes. Using a combination of molecular genetic and embryological studies, we show that a^x/a^x embryos die in the peri-implantation period 2−3 days after SAH hydrolase (SAHase) is first expressed. The use of an SAHase inhibitor or conditions that produce increased cellular levels of SAH in non-mutant embryos results in an inhibition of inner cell mass proliferation and differentiation, suggesting that loss of the *Ahcy* gene is responsible for a^x-associated peri-implantation lethality.

Results

A deletion in the a^x allele has a breakpoint close to the 3′ end of the agouti gene

The a^x mutation was detected among the offspring of an X-irradiated (C3H/R1 × 101/R1)F_1 male, therefore the mutated allele may have been either *A* or A^W (Russell *et al.*, 1963; Siracusa, 1991). Previous genetic studies have placed a^x centromere-distal to the A^y mutation by 0.12 cM (Siracusa *et al.*, 1987), and we have found recently that A^y appears to be caused by a deletion that lies centromere-proximal to the protein-coding exons of the *agouti* gene (Figure 9 and D.M.J.Duhl and G.S.Barsh, submitted). Unlike the A^y mutation, which leads to the expression of an *agouti* RNA that is slightly larger than normal in nearly every tissue of the body (Miller *et al.*, 1993), an RNA of approximately normal size is present in the testis of a^x/a mice, but in no other tissues we examined (Figure 1). Taken together, these observations suggested that the molecular lesion responsible for the a^x mutation was a deletion or subchromosomal rearrangement with a breakpoint that lay close to, but not within, *agouti* protein-coding sequences.

To detect restriction fragment length variants (RFLVs) associated with a putative a^x breakpoint, we performed a series of Southern hybridization experiments with genomic DNA from mice that carried the a^x allele opposite one of several other *agouti* alleles. Four DNA fragments that sampled a 60 kb contig spanning the *agouti* gene (designated 'a−d', Figure 2B) were used as hybridization probes. With probe c, which contains a portion of *agouti* exon 4, a 16 kb *Bcl*I RFLV and a 10 kb *Bam*HI RFLV were observed in a^x/a^t but not in a^t/a^t mice (Figure 2A). These fragments were not observed with mice carrying other *agouti* locus alleles including FVB/N-*A*/*A*, 129/Sv-A^W/A^W and C57BL/6J-$A^{W\text{-}J}/A^{W\text{-}J}$ (data not shown), and are therefore specific for the a^x allele. No a^x-specific RFLVs were detected with the other probes, although an *a*-specific *Bam*HI RFLV was detected by probe b, which allowed us to determine that the 5′ region of the *agouti* gene is not deleted from the a^x-chromosome (data not shown).

Analysis of DNA from mice that carried either the a^x or a^t allele opposite an *A* allele derived from *Mus castaneus* indicated that the area represented by probe d, located ~20 kb centromere-distal to *agouti* protein-coding sequences, was deleted from the a^x chromosome (Figure 2A). Together with the results obtained using probes b and c, these findings indicate that at least 20 kb are deleted from the a^x chromosome, with a proximal inhibition close to the most 3′ exon of *agouti*. Because the deletion is not present in any other *agouti* alleles we analyzed, including *A* and A^W, it is likely to represent the molecular lesion responsible for the a^x mutation.

The a^x allele contains a 100 kb deletion

To characterize further the molecular nature of the a^x deletion, we cloned an a^x-specific restriction fragment predicted to contain the deletion breakpoint junction defined by probes c and d (Figure 2C). A size-selected *Bcl*I subgenomic library was prepared from DNA of a^x/a mice, and screened with a probe that contained *agouti* coding sequence. Four independent clones were recovered, which were identical as judged by their restriction fragment patterns, and are described as λax. Further restriction map analysis and subcloning suggested that the breakpoint detected by probes b and c was located 4 kb centromere-distal of *agouti* exon 4 (Figure 2B and C) within a 1.5 kb *Pst*I fragment of λax. The sequence of the centromere-proximal end of this *Pst*I fragment was identical to the corresponding region from an A^W except for a single nucleotide difference (Figure 2D). The breakpoint was determined to lie at the sequence CTGAC|TTACG, ~250 nucleotides centromere-distal to the *Pst*I site. The corresponding region from the A^W chromosome, CTGAG|AGGAA, did not contain any repetitive elements or unusual features (Figure 2D, data not shown).

To investigate whether the breakpoint contained within the a^x-specific 16 kb *Bcl*I fragment was part of a more complex rearrangement, we hybridized DNA probes from the proximal and distal sides of this fragment to high molecular weight restriction fragments generated by digestion with *Mlu*I, *Not*I, *Sal*I or combinations of these enzymes, and separated by CHEF electrophoresis. A portion of probe c was used to detect the proximal side of the a^x breakpoint; and a 1.2 kb *Stu*I−*Pst*I fragment designated probe e was used to detect the distal side of the a^x breakpoint. In DNA from *a/a* mice digested with *Not*I or *Not*I + *Mlu*I, the same 940 kb or 600 kb fragments, respectively, are detected by both probes (Figure 3A), showing that the proximal and distal portions of the a^x breakpoint junction are normally separated by no more than 600 kb. In DNA from *a/a* mice digested with *Sal*I or *Not*I + *Sal*I, probes c and e detect the same 560 kb and 580 kb fragments, but probe c detects 380 kb and 400 kb fragments not detected by probe e, while

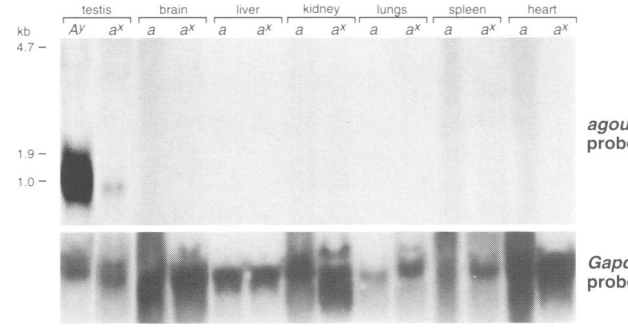

Fig. 1. Expression of *agouti* coding sequences in tissues of a^x/a and *a/a* mice. Total RNA (30 μg) from the indicated tissues was fractionated by formaldehyde−agarose gel electrophoresis, transferred to a nylon filter and hybridized with a probe that contains *agouti* exons 3 and 4. The filter was also hybridized with a *Gapd* 'housekeeping' probe to control for the amount and integrity of the RNA. Tissues were from adult mice of genotypes A^y/a^x, a^x/a or *a/a* (designated 'A^y', 'a^x' or '*a*', respectively). The A^y/a^x testis sample served as a positive control and represents a mixture of chimeric RNAs between 0.9 and 1.2 kb in length that have different 5′ ends, but which all contain *agouti* exons 2, 3 and 4 at the 3′ end.

probe e detects a 180 kb fragment not detected by probe c. This indicates the presence of two *Sal*I sites that are partially digested; one that separates probe c from probe e, and a second that lies on the centromere-proximal side of the fragment that contains probe c. The presence of these *Sal*I sites was confirmed by analysis of *a/a* DNA digested with *Sal*I + *Mlu*I, in which probes c and e detect the same 520 kb fragment, probe c detects a 340 kb fragment not detected by probe e, and probe e detects a 180 kb fragment not detected by probe c. The fragment sizes, summarized in Table I, are consistent with the results of additional hybridizations with centromere-proximal probes (data not shown). These results allow the construction of a long range restriction map for the *a* chromosome (Figure 3B), and indicate that the a^x breakpoint junction (Figure 2B) does not involve an insertion or inversion, but instead can be explained by a simple deletion.

To estimate the size of the a^x deletion, we constructed a long-range restriction map of the a^x chromosome by comparing the patterns produced from a^x/a DNA with those from *a/a* DNA (Figure 3B). As expected, the a^x-specific fragments detected by probes c and e were identical (Figure 3A, Table I). Although multiple fragments were observed in *a/a* DNA digested with *Not*I + *Sal*I, *Sal*I or *Sal*I + *Mlu*I, these enzymes generated a smaller number of a^x-specific fragments (Figure 3A, Table I). The pattern of the a^x-specific fragments suggested that the partially cleaved *Sal*I site separating probes c and e had been deleted from the a^x chromosome (Figure 3B). The a^x-specific *Sal*I and *Sal*I + *Mlu*I fragments, 460 kb and 420 kb, respectively, are 100 kb smaller than their counterparts in the *a* chromosome, 560 kb and 520 kb. However, the a^x-specific *Not*I, *Not*I + *Mlu*I and *Not*I + *Sal*I fragments are 220 kb smaller than their counterparts in the *a* chromosome. This apparent inconsistency in the estimated size of the a^x deletion is most likely due to the presence of a variant *Not*I site in the a^x but not in the *a* chromosome (indicated with an asterisk in Figure 3B), since a *Not*I site lies in a similar position in the A^y chromosome (data not shown). These results indicate that probes c and e are separated normally by ~100 kb, and that this section of DNA has been deleted from the a^x chromosome (Figure 3B).

The a^x deletion includes a gene involved in SAH metabolism

During the course of analyzing DNA fragments from the contig that spanned the *agouti* gene, we determined the sequence of a 1.4 kb *Eco*RI fragment at the centromere-distal end of the contig. This fragment, designated probe d in Figure 2, attracted interest originally because it appeared to contain a CpG island as judged by restriction map analysis of cloned DNA. Sequence analysis demonstrated that it was a CpG island, and similarity searches revealed a segment in which 35 of 37 nucleotides matched the 5′ end of the human cDNA for *Ahcy*, including the first nine codons (Figure 4; Coulter-Karis and Hershfield, 1989). At the point where similarity ended between the mouse genomic and human cDNA sequences, a potential splice donor site, CG|gtgagt, was found in the mouse genomic sequence. The *Ahcy* gene has been mapped to human chromosome 20

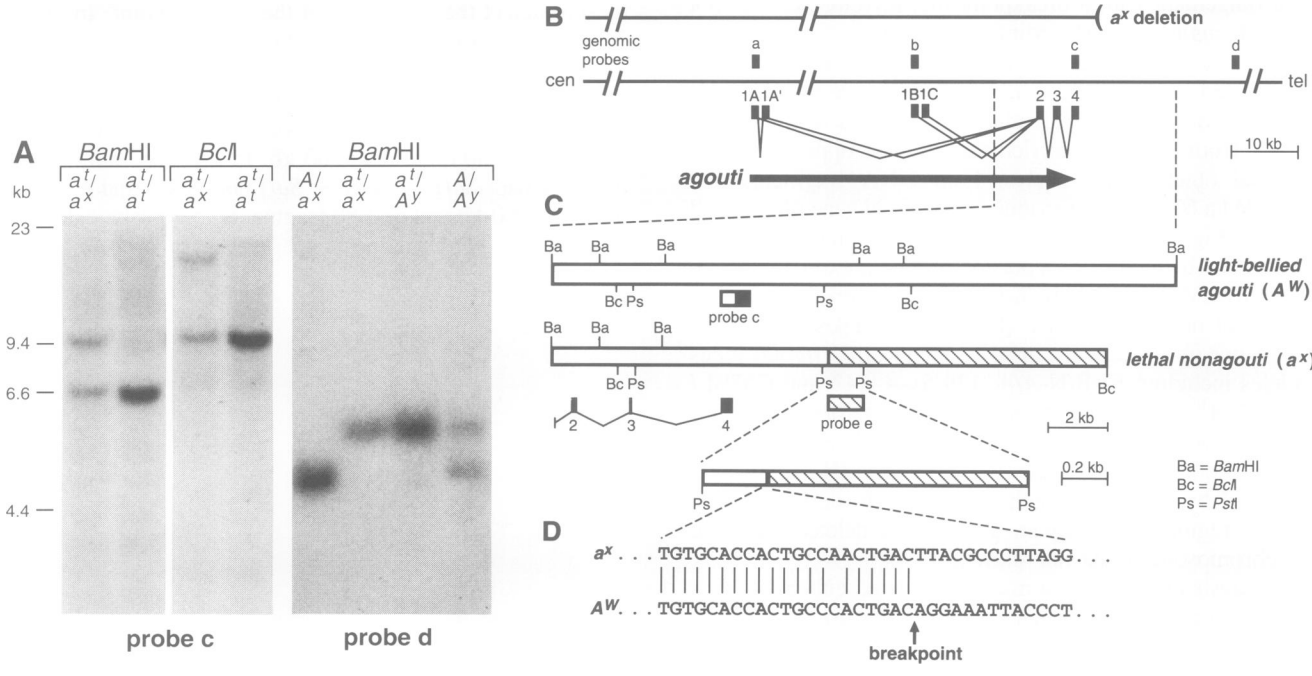

Fig. 2. Location, map and sequence of the a^x deletion breakpoint junction. (**A**) Genomic DNA from a^t/a^x, a^t/a^t, a^t/A^y, A/a^x or A/A^y animals, in which the *A* allele was derived from *M.castaneus*, was digested with *Bam*HI or *Bcl*I, fractionated on an agarose gel, and transferred to a nylon filter. Probe c detects an a^x-specific RFLV for both enzymes, and probe d is deleted from the a^x chromosome. (**B**) Genomic structure of *agouti* and location of the proximal a^x deletion breakpoint. The alternative first exons of *agouti* (1A, 1B and 1C) represent different promoters that are regulated in a region- and temporal-specific fashion (H.Vrieling and G.S.Barsh, in preparation). The distance between exon 1A′ and 1B is ~100 kb. (**C**) An enlargement of the centromere-proximal a^x deletion breakpoint site, and restriction maps comparing the A^W and the a^x chromosomes. The 16 kb a^x-specific *Bcl*I fragment detected by probe c was cloned as a recombinant bacteriophage as described in Materials and methods (λax), and part of a 1.5 kb *Pst*I fragment that spanned the breakpoint junction was sequenced. Probe e represents the distal portion of the breakpoint junction. (**D**) DNA sequence of the breakpoint junction compared with the corresponding region from an A^W chromosome. The a^x and the A^W sequences are identical for an additional 250 nucleotides centromere-proximal to the breakpoint.

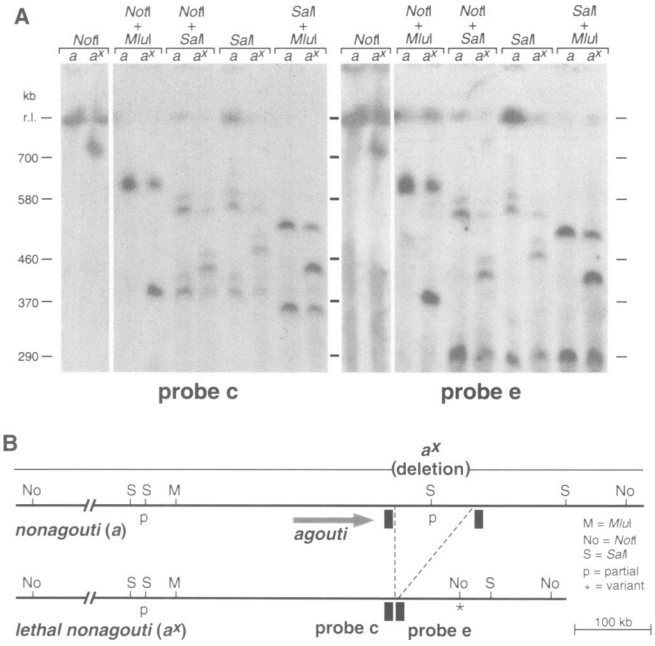

Fig. 3. CHEF gel electrophoresis analysis of DNA from *a/a* and a^x/a mice. (**A**) DNA from *a/a* (indicated as '*a*') or a^x/a (indicated as 'a^x') mice was digested with the indicated restriction enzyme or enzyme combinations, fractionated by CHEF electrophoresis as described in Materials and methods, and a Southern blot hybridized with probes which originate from proximal and distal portions of the a^x deletion breakpoint junction. r.l., resolution limit. The fragment described as 'probe c' for the hybridizations shown here is a 500 bp *Bss*HII–*Eco*RI fragment that represents the centromere-distal half of the fragment described as 'probe c' and used for the hybridization shown in Figure 2A. Removal of residual probe between hybridizations was checked by autoradiography. The results obtained for *Not*I are from a different experiment from those obtained for *Not*I + *Mlu*I, *Not*I + *Sal*I, *Sal*I and *Sal*I; this latter experiment also included lanes for A^y/a^x DNA which are not shown in the figure. (**B**) Long range restriction map for the *a* and a^x chromosomes based on the results shown in (A). The size of the *a/a Not*I fragment, 940 kb, is based on separate experiments. A variant *Not*I site present in the a^x and not the *a* chromosome is marked with an asterisk, and the a^x deletion of 100 kb is centered arbitrarily at the partially cleaved *Sal*I site contained within the deletion. Both the variant *Not*I site and the partially cleaved *Sal*I site are found in association with the A^y allele (data not shown). The relative positions of the centromere-proximal *Mlu*I and *Not*I sites and the sizes of the corresponding restriction fragments are consistent with those previously described for a centromere-proximal probe from the *Parotid secretory protein* (*Psp*) gene (Barsh and Epstein, 1989a; Siracusa, 1991).

cen-20q31 (Hershfield and Francke, 1982; Mohandas *et al.*, 1984), which lies in a region of conserved synteny with mouse chromosome 2 (Siracusa and Abbott, 1992). Furthermore, sequences similar to the rat *Ahcy* gene lie in the same subchromosomal region as *agouti* (Pilz *et al.*, 1992; L.Siracusa, personal communication). Thus, it seemed likely that the 1.4 kb *Eco*RI fragment at the centromere-distal end of the contig spanning *agouti* contained the first exon of the mouse *Ahcy* gene, and that mouse *agouti* and mouse *Ahcy* were located next to each other and transcribed in opposite directions.

To confirm that the contig spanning *agouti* contained sequences similar to the *Ahcy* gene and to determine the approximate length of the mouse *Ahcy* gene, we used a full-length human *Ahcy* cDNA as a hybridization probe to examine the *agouti* contig. Cross-hybridization with *Ahcy* sequences was localized to a 9.4 kb *Bam*HI fragment that

Table I. High-molecular-weight restriction fragments detected by probes from the a^x deletion breakpoint junction[a]

Probe	*Not*I		*Not*I + *Mlu*I		*Not*I + *Sal*I		*Sal*I		*Sal*I + *Mlu*I	
	a	a^x	*a*	a^x	*a*	a^x	*a*	a^x	*a*	a^x
c	940[b]	720	600	380	580	440	580	480	520	420
					560	420	560	460	340	
					400		400			
					380		380			
e	940[b]	720	600	380	580	440	580	480	520	420
					560	420	560	460	180[c]	
					180[c]		180[c]			

[a]Estimated sizes are in kb based upon the results shown in Figure 3, and are consistent with both the mobility of yeast chromosomes in adjacent lanes and with the construction of an internally consistent restriction map. Two exceptions are noted below. Probes c and e lie on centromere-proximal and centromere-distal sides of the a^x deletion breakpoint and are described fully in the Results and in Figure 2. Comparison of the fragments observed in the *a/a* and a^x/a DNA samples allowed us to determine their chromosomal origin as '*a*' or 'a^x'.

[b]This fragment has an electrophoretic mobility above the limit of resolution shown in Figure 3 and its estimated size is based on the results of other experiments.

[c]This fragment exhibited an aberrantly slow electrophoretic mobility in the results shown in Figure 3. Its estimated size of 180 kb is based on the results of other experiments and on the sizes of other *Sal*I fragments in the *a/a* sample.

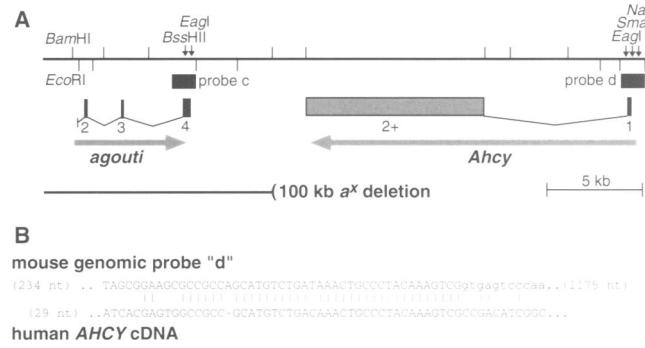

Fig. 4. Location of the *Ahcy* and *agouti* genes in the vicinity of the a^x deletion. (**A**) Genomic restriction map of the area including the translated exons of the *agouti* gene, the a^x deletion breakpoint and the entire *Ahcy* gene. The *Ahcy* exons other than the first are located within the 9.4 kb *Bam*HI fragment, but exact positions are not yet known. (**B**) Comparison of the mouse genomic DNA sequence from probe d with the human AHCY cDNA sequences. Endpoints for the mouse genomic sequence are *Eco*RI sites at the ends of probe d. The numbering for the human cDNA sequence is taken from Coulter-Karis and Hershfield (1989). The point where the mouse genomic and human cDNA sequences diverge contains a consensus splice donor site and is indicated by a change from upper case to lower case letters.

lay 3′ to *agouti* coding sequences (Figure 4 and data not shown) suggesting that the entire mouse *Ahcy* gene was contained within a 20 kb region whose centromere-proximal end was located 6 kb centromere-distal to the 3′ end of the *agouti* gene.

We have described previously another cDNA close to the 3′ end of the *agouti* gene, designated '0252', which, like *Ahcy*, has a transcriptional orientation opposite to that of *agouti* (Miller *et al.*, 1993). The '0252' cDNA detects a 6 kb RNA in the testes, and in 2.1 kb of sequence from the 3′ end, does not contain a significant open reading frame. We

considered whether this 6 kb RNA might represent an alternatively spliced form of *Ahcy*; however, the human *Ahcy* cDNA probe detects a smaller RNA on Northern blots from mouse tissues, and does not hybridize with the 6 kb testis RNA detected by the '0252' cDNA (data not shown).

Functional analysis of SAHase and ADA activity in a^x/a mice

SAHase catalyzes the reversible hydrolysis of SAH (produced from SAM in all transmethylation reactions) to adenosine and homocysteine (De La Haba and Cantoni, 1959; Walker and Duerre, 1975), is found in all eukaryotes, and is highly conserved (Ogawa *et al.*, 1987; Kasir *et al.*, 1988; Coulter-Karis and Hershfield, 1989; Henderson *et al.*, 1992; Prasad *et al.*, 1993). However, there are several *Ahcy* pseudogenes in humans (data not shown); thus, the deletion of *Ahcy*-related sequences from the a^x mutant chromosome suggests but does not prove that the enzymatic activity is ablated in mice that carry the mutant allele. Because a^x/a^x embryos do not survive much beyond implantation, it is not possible to assay for the protein in homozygous mutant tissues. Therefore to test more directly for loss of SAHase, we measured its activity in adult a^x/a and a/a mice, using adenosine deaminase (ADA) activity as a control. Comparing a^x/a versus a/a animals, measurements from homogenates of erythrocytes, liver and spleen found SAHase activity to be reduced by 43 and 53%, respectively, in a^x/a animals (Table II). These results are consistent with heterozygosity for a null allele, and, together with the results presented above, confirm that the mouse *Ahcy* gene has been deleted in the a^x mutation.

Table II. SAHase and ADA activity in a^x/a versus a/a mice[a]

Organ	Genotype	Animal	SAHase (nmol/h/mg)	ADA (nmol/h/mg)
Red blood cells	a^x/a	1	6.30	129
		2	5.91	135
		3	5.55	144
		mean	**5.92 ± 0.37**	**136 ± 7**
	a/a	4	11.9	101
		5	8.46	91.8
		6	10.4	107
		mean	**10.3 ± 1.7**	**100 ± 8**
Liver	a^x/a	1	767	377
		2	847	347
		3	942	384
		mean	**852 ± 88**	**369 ± 20**
	a/a	4	1818	430
		5	1463	460
		6	ND	ND
		mean	**1641**	**445**
Spleen	a^x/a	1	82.7	3710
		2	101	5180
		3	113	6010
		mean	**98.9 ± 15.3**	**4970 ± 1170**
	a/a	4	185	3710
		5	241	4710
		6	ND	ND
		mean	**213**	**4210**

[a]Each sample was assayed in triplicate and only the mean values are shown. The mean values for all three animals of each genotype are indicated in bold.
ND, not determined.

Developmental potential of a^x/a^x homozygotes and expression of SAHase

A previous study by Papaioannou and Mardon (1983) suggested that a^x/a^x embryos first appear abnormal at 4.5 days post-coitum (d.p.c.) around the time of implantation. However, at the time these experiments were performed, it was not possible to correlate the genotype of individual embryos with specific morphologic abnormalities. To determine when a^x/a^x embryos die, we made use of an RFLV closely linked to the *agouti* locus (Lovett *et al.*, 1987; Siracusa *et al.*, 1989; Miller *et al.*, 1993) to determine the genotype of individual embryos and animals recovered at different times from an $a^x/a \times a^x/a$ intercross. Of 65 pre-implantation embryos (42 blastocysts and 23 blastocyst outgrowths), 19 (29%) were a^x/a^x homozygotes (Table III). However, of 44 post-implantation embryos (including 29 examined at 6.5 d.p.c.), no a^x/a^x homozygotes were found, indicating that a^x-associated lethality is likely to occur in the peri-implantation period between 4.5 and 5.5 d.p.c..

To evaluate whether SAHase was expressed in embryonic material corresponding to this developmental stage, we examined undifferentiated embryonic stem cells in culture, which resemble primitive ectoderm tissue of the embryo (Rossant and Papaioannou, 1984). Embryonic stem (ES) cells were stained with a mixture of monoclonal antibodies raised against human SAHase that recognize mouse SAHase, and then stained with a fluorescent secondary antibody. Diffuse cytoplasmic immunofluorescence was observed in small groups of clustered ES cells (Figure 5A), with weaker staining observed in embryonic fibroblasts of the underlying feeder layer. In control samples which did not include the primary antibody, only a low level of background staining of the ES cells was apparent (Figure 5A).

We were unable to examine pre-implantation embryos with anti-SAHase antibodies due to high levels of background staining, possibly from mouse immunoglobulin present in the maternal reproductive tract. However, we investigated whether *Ahcy* RNA was present using an RT-PCR assay. RNA from ~25 unfertilized eggs, 25 two-cell embryos, or

Table III. Development of embryos derived from an $a^x/a \times a^x/a$ intercross[a]

	Genotype[b]			
	a/a	a^x/a	a^x/a^x	Total
Blastocysts	10	20	12	42
Outgrowth	6	10	7	23
Total	16 (25%)	30 (46%)	19 (29%)	65
E6.5	7	22	0	29
E9.5	4	11	0	15
Liveborn	10	18	0	28
Total	21 (29%)	51 (71%)	0	72

[a]3.5 d.p.c. blastocysts were obtained as described in Materials and methods and placed into *in vitro* culture. As embryos attached and formed outgrowths during the next 2 days, they were scraped from the dish and prepared for genotyping. Post-implantation embryos at E6.5 and E9.5 were dissected from maternal decidua.
[b]The *agouti* genotype of each embryo was inferred from the identity of a variant *Hin*dIII site at the closely linked *Emv-15* locus as described in Frohman *et al.* (1993). It was possible to correlate genotype and phenotype for three of the a^x/a^x outgrowths recovered after 2 days in culture (corresponding to E5.5). Two embryos had attached and had not formed any inner cell mass and the third embryo had a smaller inner cell mass.

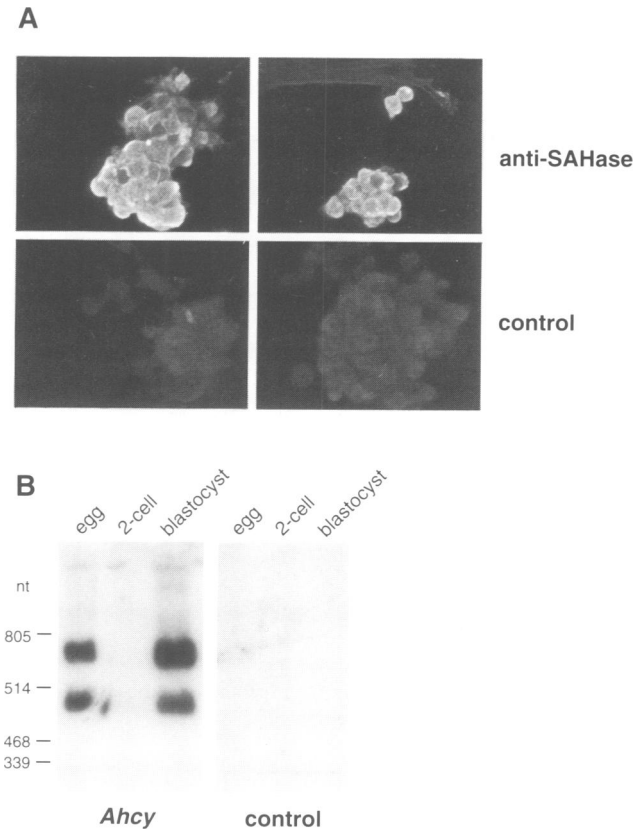

Fig. 5. Expression of SAHase protein in embryonic stem cells and SAHase RNA in pre-implantation embryos. (**A**) R1 embryonic stem cells were stained with monoclonal antibodies against SAHase as described in Materials and methods and photographed at 400× using laser confocal microscopy to detect a fluorescein signal. The primary antibodies were not included for the control specimens. Two panels taken from different areas of the slide are shown for the anti-SAHase antibody and control samples. (**B**) RNA from C57BL/6J unfertilized eggs or embryos was reverse transcribed and PCR-amplified with oligonucleotide primers specific for *Ahcy* as described in Materials and methods. For a negative control (shown in the right panel), a parallel aliquot of the same RNA reverse transcribed with an unrelated oligonucleotide was PCR-amplified with *Ahcy* primers. The PCR-amplified material was fractionated by gel electrophoresis, transferred to a nylon membrane and hybridized with an internal oligonucleotide probe specific for *Ahcy*. The expected product is 662 bp; the smaller product has not been characterized.

five blastocysts was reverse transcribed with an antisense oligonucleotide primer complementary to rat and human *Ahcy* coding sequence and then PCR-amplified using a sense primer from mouse *Ahcy* exon 1. In the samples from unfertilized eggs and blastocysts, a fragment of the expected size, 662 bp, hybridized to an internal oligonucleotide probe from rat and human *Ahcy* coding sequences (Figure 5B), suggesting that both maternal and embryonic *Ahcy* RNA may be present prior to the time that a^x/a^x embryos die. A smaller fragment of ~500 bp that also hybridized with an internal oligonucleotide probe has not been characterized, but may result from alternative splicing of the *Ahcy* gene or from an expressed *Ahcy* pseudogene.

Elevated cellular SAH levels affect development of the inner cell mass

SAH is produced by all SAM-dependent transmethylation reactions including those that affect proteins, nucleic acids and small molecules such as creatine. Efficient hydrolysis

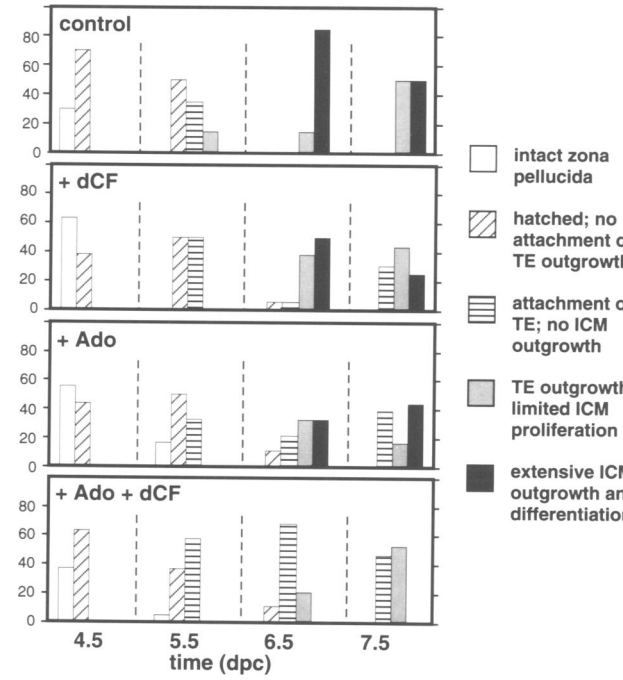

Fig. 6. Effects of adenosine and dCF on non-mutant embryos *in vitro*. Blastocysts obtained from superovulated FVB/N mice were placed into microdrop cultures of either control medium (26 embryos), or the same medium containing either dCF (23 embryos), Ado (22 embryos) or Ado + Hcy + dCF (31 embryos) as described in Materials and methods. Embryos were photographed daily (see Figure 7 for examples), and categorized within the five conditions shown on the right as described in Materials and methods. Bars represent percentages (shown on the abscissa) of embryos in each condition, each day and each media.

of SAH by SAHase is required to maintain a normal ratio of SAM to SAH, which is >10 in most cells and tissues, and is sometimes referred to as the methylation index since elevated levels of SAH inhibit virtually all methyltransferases (Salvatore *et al.*, 1977; Borchardt *et al.*, 1982). Inhibition of SAHase leading to decreased methylation and cellular toxicity has been studied extensively in cultured cells using a variety of adenosine analogs (Greenberg *et al.*, 1989; Cools and De Clercq, 1990; Chiang *et al.*, 1992; Duerre *et al.*, 1992). To determine whether elevated levels of SAH in pre-implantation embryos could account for a^x-associated lethality, we used two different approaches.

First, 20–30 d.p.c. blastocysts were cultured in the presence of media supplemented with adenosine and/or 2′-deoxycoformycin (dCF), an ADA inhibitor. The rationale for this approach was based on studies of ADA-deficient lymphoblasts, in which elevated cellular levels of adenosine produce increased SAH levels both by driving the SAHase-catalyzed reaction towards the formation of SAH and by the deoxyadenosine-induced irreversible inactivation of SAHase (Hershfield, 1979; Kredich and Hershfield, 1979, 1989). By themselves, 50 μm adenosine or 2 μM dCF had no detectable effect on cultured blastocysts (Figure 6). Together, adenosine plus dCF did not affect general embryo viability, hatching from the zona pellucida, or attachment and the formation of trophoblastic outgrowths (Figure 6), all of which occurred within 2–3 days after being placed into culture. However, by 4–5 days, embryos exhibited a specific inhibition of inner cell mass proliferation and differentiation (Figure 6).

In a second experiment, 20–30 3.5 d.p.c. blastocysts

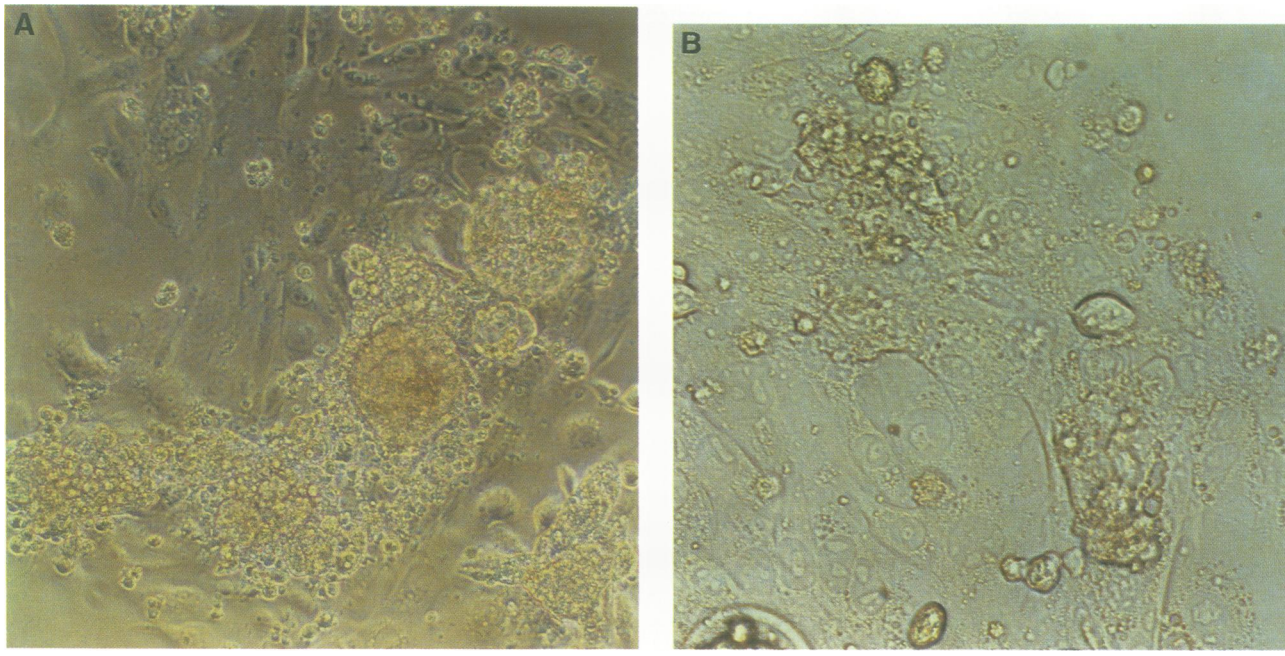

Fig. 7. Effects of an SAHase inhibitor on non-mutant embryos *in vitro*. A group of five or six embryos used for the experiment described in Figure 6. Control medium at 8.5 d.p.c. (**A**). (**B**) Medium with 20 μM 3′-deazaaristeromycin. Photographed at 400×.

were cultured in the absence or the presence of different concentrations (0.5−20 μM) of a specific SAHase inhibitor, 3′-deazaaristeromycin, and the development of each embryo was assessed for the next 4 days. Similar to the studies with adenosine and dCF, 3′-deazaaristeromycin did not affect viability, hatching or attachment, but by 4−5 days of culture, embryos exhibited an inhibition of inner cell mass proliferation and differentiation that was dependent on the concentration of 3′-deazaaristeromycin (Figures 7 and 8).

Discussion

Of the many recessive lethal mutations that affect mouse development, most are recognized because of a visible effect in heterozygotes. However, many such mutations have been induced by agents that can affect more than one gene, and it can be problematic to determine whether the heterozygous and homozygous phenotypes have the same molecular basis. At the *agouti* coat color locus, there are at least five embryonic lethal mutations—a^{jl}, a^{16H}, A^y and a^x (reviewed in Siracusa, 1991). A^y and a^x have been described as pseudoalleles, since these mutations can recombine, yet both affect *agouti* coat color (Russell *et al.*, 1963; Wallace, 1965). Here we report that a^x is caused by a 100 kb deletion that lies close to, but not within, *agouti* coding sequences, which suggests that regulatory sequences required for normal expression of *agouti* lie in the 3′ flanking region. The deletion removes the coding sequences for SAHase, which degrades an obligatory product and inhibitor of all transmethylation reactions. We have shown that SAHase is normally expressed prior to the time at which a^x/a^x embryos die at 4.5−5.5 d.p.c., and that inhibition of SAH hydrolysis in cultured blastocysts causes a specific inhibition of inner cell mass development, which suggests that loss of SAHase is likely to be the cause of a^x-associated periimplantation lethality. Taken together with recent observations regarding the molecular basis of the A^y mutation

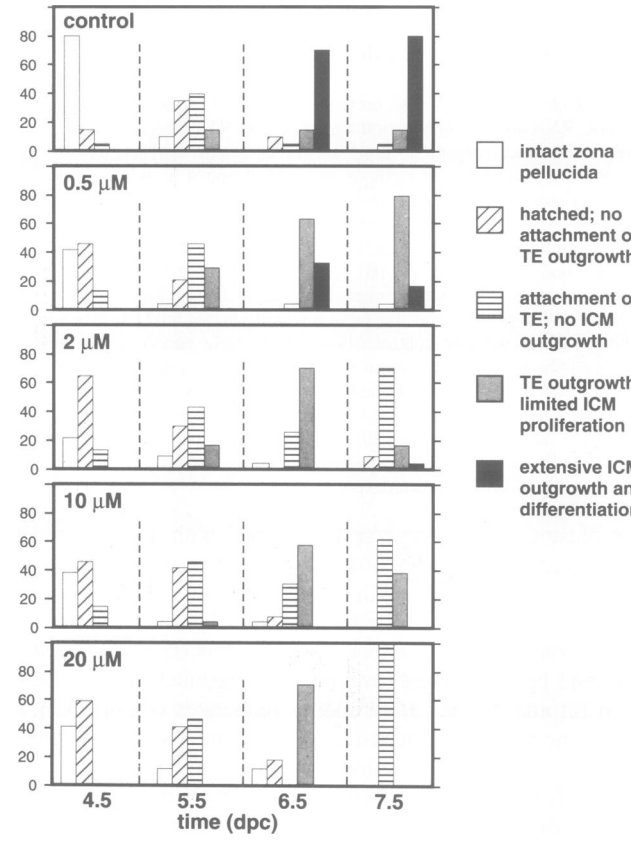

Fig. 8. Effects of an SAHase inhibitor on non-mutant embryos *in vitro*. Blastocysts obtained from superovulated FVB/N mice were placed into microdrop cultures of either DMEM supplemented with 10% fetal calf serum (control, 24 embryos), or the same medium to which 3′-deazaaristeromycin has been added to final concentrations of 0.5 μM (25 embryos), 2 μM (25 embryos), 10 μM (29 embryos) or 20 μM (20 embryos). Embryo conditions were evaluated as in Figure 6.

(D.M.J.Duhl and G.S.Barsh, submitted), our findings also help to understand pseudoallelism of a^x with A^y.

The a^x deletion and its effects

Radiation-induced mutations frequently remove large regions of DNA, and can produce complex rearrangements that involve multiple breakpoints (Rinchik *et al.*, 1986, 1993). Using probes derived from the centromere-distal side of the a^x breakpoint junction, our results demonstrate that the a^x mutation was caused by a simple deletion, with an estimated size of 100 kb. Our findings are consistent with previous studies which have shown that the markers *Emv-15* and *Xmv-10*, located 0.31 and 0.93 cM distal to *agouti*, respectively, are not deleted from a^x (Lovett *et al.*, 1987; Barsh and Epstein, 1989b; Siracusa *et al.*, 1989; Winkes *et al.*, 1994), and that a^x neither enhances nor suppresses recombination between itself and more distal markers (Russell *et al.*, 1963; Miller *et al.*, 1993).

Several observations argue that the deletion we identified which lies 4 kb centromere-distal to the last exon of *agouti*, is solely responsible for the effects of a^x on *agouti* coat color and peri-implantation development. First, the deletion is not present on either of the two possible a^x parental chromosomes, A or A^W. Second, loss of the *Ahcy* gene is sufficient to explain a^x-associated embryonic lethality, and the loss of putative 3′ flanking sequences required for normal expression of *agouti* is consistent with the hypomorphic nature of a^x coat color (see below). Finally, the observation that an A^y-a^x recombinant chromosome exhibits reversion of both a^x coat color and embryonic lethality (Russell *et al.*, 1963) indicates that the lesion responsible for a^x must lie distal to the A^y deletion breakpoint, which is located 100 kb centromere-proximal to the translational start of *agouti* (see below).

Effect of the a^x deletion on agouti expression and origin of the a^x mutation

Of the tissues we examined, *agouti* RNA was detectable by Northern analysis only in the testes of a^x/a animals. The umbrous phenotype of these animals (a non-agouti dorsum with dark agouti flanks and ventrum) indicates that a^x is a hypomorphic rather than an amorphic mutation. This suggests that positive regulatory sequences required normally for *agouti* expression may lie close to the 3′ end of the gene and are removed by the a^x deletion. Alternatively, the deletion may place the *agouti* gene next to a region of chromatin that has a negative effect on expression. The latter explanation is consistent with the observation that the effect of a^x becomes more apparent with age: both the proportion of ventral banded hairs and the intensity of phaeomelanin within the band increase with successive hair growth cycles (Galbraith *et al.*, 1979). Such a negative effect would not be a general one, however, given that the a^x deletion does not affect expression of *agouti* in the testis.

Recently, we found that two distinct promoters control *agouti* transcription: one that lies close to *agouti* coding sequences directs expression throughout the entire hair growth cycle but only in the ventral region of the body ('the ventral-specific promoter'); and a second that lies 100 kb further away directs expression in both the dorsum and the ventrum but only in the mid-portion of the hair growth cycle ('the hair cycle-specific promoter') (Vrieling *et al.*, 1994). Both promoters are active in the wild-type *light-bellied agouti*

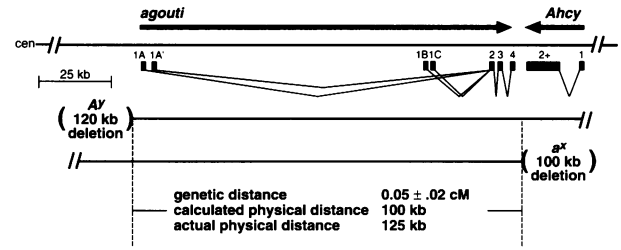

Fig. 9. Location of the A^y and a^x deletions relative to *agouti* coding sequences. Mapping of the A^y deletion and the genomic structure of *agouti* will be described fully elsewhere (D.M.J.Duhl and G.S.Barsh, submitted). The value for genetic distance between A^y and a^x is based on a combination of results from $A^y/a^x \times A^y/a^x$ intercrosses: Siracusa *et al.* (1987) reported five recombinants in 3784 progeny; and one of us (G.L.Wolff) has observed no recombinants among 7084 progeny. The calculated physical distance is based on an average of 2000 kb/cM for the mouse genome, and the actual physical distance has been determined by construction of a *Bam*HI restriction map.

(A^W) allele, and reduced expression from the ventral-specific promoter explains the phenotype of the *agouti* (A) allele. The a^x mutation was induced in a (C3H/R1 × 101/R1)F_1 animal, and, a priori, may have originated from either A or A^W. However, since the ventral-specific promoter in A^y-a^x recombinants originates from the a^x chromosome, the phenotype of these recombinants, agouti rather than light-bellied agouti, suggests that a^x originated from an A allele (Russell *et al.*, 1963), and is consistent with the single nucleotide difference we observed between the A^W and a^x chromosomes just proximal to the a^x deletion breakpoint.

a^x and other recessive lethal agouti mutations

The recessive lethal mutations of a^x, A^y, a^{16H} and a^l can be divided into three complementation groups represented by a^x, A^y and a^{16H}. Michaud *et al.* (1993) have demonstrated that a gene likely to encode an RNA binding protein, *Raly*, is deleted from the A^y chromosome, and we have found that A^y is a deletion similar to size to a^x, but located 125 kb away towards the centromere (D.M.J.Duhl and G.S.Barsh, submitted). The locations of the A^y and a^x deletions centromere-proximal and distal, respectively, to *agouti* coding sequences, help to explain not only the observation that A^y/a^x animals are viable, but also the pseudoallelism of these mutations (Russell *et al.*, 1963; Wallace, 1965; reviewed in Siracusa, 1991). Based on an average of 2000 kb/cM for the mouse genome, a genetic distance of 0.05 ± 0.02 cM corresponds to 100 kb, which is relatively close to the 125 kb that separates the A^y and a^x deletions (Figure 9).

Besides A^y, a^x is viable in combination with a^{16H}, an ethylnitrosourea-induced mutation with a hypomorphic coat color phenotype similar to a^x (Barsh and Epstein, 1989b; Siracusa, 1991). a^{16H}/A^y animals are viable, which might suggest that the molecular lesion in a^{16H} lies between the A^y and a^x deletions. However, a^{16H}/a^l animals are also viable, yet A^y/a^l and a^x/a^l animals are not. This apparent complementation of a^{16H} and a^l is difficult to explain unless the molecular lesions in one or both of these mutations affect non-contiguous genes. This may indeed be the case for a^{16H}, since in the original description of a^{16H}, the proportion of a^{16H}/a^l progeny was less than expected in some crosses, and since the effect of a^{16H} on agouti coat color can be separated by recombination from the effect on embryonic

viability (G.S.Barsh and C.J.Epstein, unpublished data).

Lack of complementation between a^x and a^l indicates that both mutations affect the same gene required for embryonic viability. We have reported previously that a^l appears to be a large deletion likely to include *agouti* coding sequences, based on long range restriction mapping using a centromere-proximal probe from the *Parotid secretion protein* (*Psp*) gene (Barsh and Epstein, 1989a,b). We argue below that loss of the *Ahcy* gene is responsible for a^x-associated peri-implantation lethality. Using probes closer to the *agouti* gene, it should now be possible to define the molecular lesion in a^l more precisely, and thus help to define the physical boundaries for a^x-associated peri-implantation lethality.

a^x-associated embryonic lethality and loss of Ahcy

The *Ahcy* gene accounts for ~20 kb of the 100 kb of DNA deleted from the a^x chromosome, and the deletion may include additional genes besides *Ahcy* that affect development or viability. However, several observations suggest that loss of SAHase activity is the critical lesion in a^x-associated embryonic lethality. In eukaryotic cells, hydrolysis by SAHase is the only pathway for degradation of SAH, which is produced in all *S*-adenosylmethionine (SAM)-dependent methyltransferase reactions (Salvatore *et al.*, 1977; Borchardt *et al.*, 1982). Accumulation of SAH inhibits these reactions and may affect a variety of processes that depend on normal transmethylation including transcriptional regulation, RNA processing and creatine synthesis (Kredich and Hershfield, 1980; Chiang *et al.*, 1992).

In cultured cells, extensive inhibition of SAHase is toxic due to inhibition of methylation reactions by elevated levels of cellular SAH (Kredich and Martin, 1977; Kredich and Hershfield, 1979; Greenberg *et al.*, 1989), which is consistent with the preliminary observation that we have been unable to derive a^x/a^x embryonic stem cells. In the embryo, loss of SAHase is likely to have its greatest impact when transmethylation reactions are abundant. Pre-implantation embryos have relatively long cell cycle times and low levels of DNA methylation, but gastrulation is associated with dramatic increases in both DNA methylation and cell proliferation (Snow and Bennett, 1978; Jaenisch and Jahner, 1984). Most important, treatment with the specific inhibitor of SAHase, 3′-deazaaristeromycin, inhibits development of the inner cell mass in cultured embryos. These effects provide an *in vitro* model for the defects we observe in a^x/a^x embryos—an ability to attach and form trophoblastic outgrowths in culture, but death *in utero* prior to 6.5 d.p.c. —and suggest that loss of SAHase is sufficient to explain the a^x/a^x mutant phenotype. The construction of transgenic mice that express SAHase should allow rescue of a^x-associated peri-implantation lethality, and may reveal whether there are additional genes within the 100 kb deletion that affect development or viability.

A variety of genetic defects might be expected to produce findings like those we observed in a^x/a^x embryos, but a review of >20 recessive lethal mutations by Magnuson (1986) included none with a similar phenotype. Because loss of SAHase affects a general aspect of cellular metabolism, a specific effect on the inner cell mass is likely caused by more rapid cell cycle times and/or increased metabolic needs of these cells *in vitro* and *in vivo*. There are few examples of potential cell-lethal mutations in other genes that can be compared with a^x in terms of the phenotype. However, it is interesting to note that absence of glycolysis caused by a null mutation in glucose phosphate isomerase results in embryonic death after implantation, between 7.5 and 8.5 d.p.c. (West *et al.*, 1990). Two other pre-implantation lethals in which molecular lesions have been identified are an inability of the trophoblast to invade the maternal decidua caused by targeted disruption of the low density lipoprotein receptor-related protein (Herz *et al.*, 1992), and failure of A^y/A^y embryos to hatch, which appears to be caused by absence of maternally expressed RNA binding protein (Michaud *et al.*, 1993; D.M.J.Duhl and G.S.Barsh, submitted). Identification of the molecular lesions responsible for additional recessive lethal mutations will help to understand when and where a particular aspect of cellular metabolism becomes important to a developing embryo.

Materials and methods

Mouse strains and mutations

Mice carrying the a^x mutation were obtained originally from Dr Virginia Papaioannou (Tufts University School of Medicine, Boston, MA) and are propagated in our laboratory as a congenic C57BL/6J-a^x/a stock by backcrossing to C57BL/6J-a/a animals obtained from The Jackson Laboratory. DNA used in the studies described here was obtained from animals afer 5–10 backcross generations. Genomic DNA from a^l/a^x, a^l/a^l, a^l/A^y, A/a^x or A/A^y animals used in the experiment shown in Figure 2 was obtained from animals in an intersubspecific backcross in which the *A* allele was derived from *M.castaneus*.

In comparing the genetic and physical distances between A^y and a^x, we use a value of 0.05 ± 0.02 cM for the genetic distance. This is based on a combination of results from $A^y/a^x \times A^y/a^x$ intercrosses: Siracusa *et al.* (1987) reported five recombinants in 3784 progeny from a stock at Oak Ridge National Laboratory; and one of us (G.L.Wolff) has observed no recombinants among 7084 progeny from an inbred strain, AX/Nctr, maintained at the National Center for Toxicological Research. The difference between the two sets of observations may reflect the different genetic backgrounds.

DNA probes, genomic cloning and sequence analysis

We generated a 150 kb contig surrounding the *agouti* gene based on previously reported results, and the restriction maps of two bacteriophage P1 clones obtained by screening a commercial library (Genome Systems, St Louis, MO) with primer pairs derived from *agouti* cDNAs or genomic clones. The structure of these P1 clones and the relative locations of *agouti* exons is described fully elsewhere (Vrieling *et al.*, 1994).

The probes shown in Figures 2 and 3 were derived from genomic DNA as follows: probe a is a 1.3 kb *Bam*HI–*Xba*I fragment that contains *agouti* exon 1A (D.M.J.Duhl and G.S.Barsh, submitted); probe b is a 0.7 kb genomic *Stu*I–*Eco*RI fragment that contains *agouti* exons 1B and 1C; probe c is a 1 kb *Xba*I–*Eco*RI fragment that contains *agouti* exon 4; and probe d is a 1.4 kb *Eco*RI fragment that lies at the centromere-distal end of the contig. Probe e, a 1.2 kb *Stu*I–*Pst*I fragment, is from the centromere-distal side of the a^x deletion breakpoint junction and was subcloned from λax (see below).

The human Ahcy cDNA, pDEC20-1, used as a probe to examine cloned and genomic mouse DNA by Southern hybridization studies is described in Coulter-Karis and Hershfield (1989).

To isolate the a^x deletion breakpoint junction, genomic DNA was digested with *Bcl*I and fractionated by agarose gel electrophoresis. The 14–27 kb size fraction was ligated to *Bam*HI arms of the bacteriophage vector λ Dash II (Stratagene, San Diego, CA) and packaged *in vitro*. Of ~2×10^5 plaques that were screened, seven positive signals were observed, four of which were used to generate a mixture of secondary plaques. The restriction patterns of six secondary clones were identical, and are referred to as λax.

The DNA sequence surrounding the a^x deletion breakpoint was determined from a 1.5 kb *Pst*I subclone of λax (see Figure 1C) and compared with the corresponding region from A^W DNA.

Northern hybridizations, Southern hybridizations and DNA sequence analysis using modified T7 polymerase and dideoxy chain termination were performed according to standard techniques using radiolabeled nucleotides and hybridization in the presence of 5 or 10% dextran sulfate.

Pulsed field electrophoresis of genomic DNA

High molecular weight DNA was prepared from homogenized spleen tissue after the cells were embedded in blocks of low-melting temperature agarose. Restriction digests were performed in a total volume of 100 μl which contained a 40 μl block of agarose and 20–40 units of restriction enzyme. Digestion was terminated with a solution of 50 mM EDTA, 50 mM Tris, pH 8, after which the blocks were placed into the wells of a 1% agarose gel, and sealed with a small amount of agarose. Contour clamped homogeneous electric field (CHEF) electrophoresis was performed using a commercial apparatus (CBS Scientific, San Diego, CA) at 150 V, in 0.5 × TBE (45 mM Tris, pH 8, 45 mM boric acid, 1 mM EDTA) and 0.1 μg/ml ethidium bromide, at 6°C. Direction of the electric field was changed according to a ramped program from 40 to 140 s, using 1 s intervals, and total electrophoresis time was ~48 h. Molecular weight estimations were based on a yeast subline derived from strain AB1380, which carries 245, 290, 370, 460, 580, 630, 700, 770, 800, 850 and 945 kb chromosomes, and a mouse yeast artificial chromosome (YAC) of 480 kb, which served as a convenient registration marker. In some experiments, ligated concatemers of bacteriophage λ also served as size markers. For the results shown in Table I, the sizes of individual fragments were first estimated by comparison with yeast markers in adjacent lanes, which provided a 'window' of approximately ±40 kb. Exact sizes within this window were then estimated by construction of an internally consistent restriction map for the *a* and a^x chromosomes.

Enzymatic assays

Erythrocytes were lysed with an equal volume of distilled water. Hemolysate (0.1 ml) was run over a 1 ml Sephadex G-25 spun column equilibrated with 25 mM Tris, pH 7.4, 15 mM KCl, 1 mM dithiothreitol and 1 mM EDTA (Greenberg *et al.*, 1989). Samples of liver and spleen were sonicated on ice in 1.5–4 vol of this buffer containing 1 mM phenylmethylsulfonyl fluoride. After microcentrifugation for 2–3 min, 0.1 ml of supernatant was run over a G-25 spun column equilibrated with sonication buffer. Activity of *S*-adenosylhomocyteine hydrolase (SAHase) was assayed as described (Hershfield, 1979) except that adenosine deaminase (ADA) was inhibited with 1 μM 2′-deoxycoformycin instead of EHNA. ADA was assayed as described (Arredondo-Vega *et al.*, 1990). Both enzyme assays were performed in triplicate for 10 min and 20 min. Protein was determined by the Lowry method (Lowry *et al.*, 1951).

Expression of SAHase RNA and protein in mouse embryos and ES cells

Expression of *Ahcy* RNA in mouse eggs and embryos was determined using a PCR-based approach. A portion of total RNA extracted from ~50 mouse eggs, two-cell embryos or 25 blastocysts as previously described (Andria *et al.*, 1992) was reverse transcribed using an oligonucleotide primer complementary to sequences in the *Ahcy* protein-coding region, 5′-ACATCACCATAGCCTGCTAC-3′, and then PCR-amplified using the same primer in combination with an oligonucleotide from the first exon, 5′-AAACTGCCCTACAAAGTCGC-3′. The identity of the 662 bp amplified product was confirmed by Southern hybridization to an internal oligonucleotide probe, 5′-GCAGCCATAGAGGTTGTC-3′. Because the sequence of mouse *Ahcy* was available only for the first exon, the other two oligonucleotides were chosen from a region of the rat *Ahcy* gene that was identical to the human *Ahcy* gene.

For SAHase immunofluorescence, undifferentiated cells from the R1 line cultured on feeder fibroblasts were plated on gelatin-coated chamber slides and allowed to attach. The cells were fixed with 1% paraformaldehyde in phosphate-buffered saline (PBS) for 20 min in a humidity chamber at room temperature, then rinsed with PBS and permeabilized by incubation in 20–80% methanol, followed by another rinse with PBS. They were then incubated overnight at 4°C with a mixture of four mouse monoclonal antibodies raised against human placental SAHase, each diluted 3:1000. The monoclonal antibodies 7G12, 3D2, 3D4 and 10D10, were developed against a mixture of native and denatured human SAHase (Hershfield *et al.*, 1985; Henderson *et al.*, 1992), and react with a single band on Western blots of cells and tissue (M.S.Hershfield, unpublished data). Control specimens were treated in a similar fashion but no primary antibody was added. The embryos and cells were then washed with 0.1% Tween 20 in PBS and incubated for 1–2 h with the secondary antibody: affinity purified and fluorescein-coupled horse anti-mouse IgG (Vector), diluted 1:600. Both primary and secondary antibodies were diluted with PBS that contained 2% horse serum/1% bovine serum albumin/0.01% sodium azide. Finally, specimens were washed with 0.1% Tween 20 in PBS, mounted with Gelvatol (Air Products), and the embryos were photographed using a Nikon Axiophot and fluorescein filters. The ES cells were photographed using laser confocal microscopy to allow the difference between experimental and control (no primary antibody) specimens to be determined more precisely.

Embryologic studies

To determine the developmental potential of a^x/a^x embryos, C57BL/6J-a^x/a animals were intercrossed in natural matings, blastocysts were recovered at 3.5 d.p.c., and placed into *in vitro* microdrop culture with DMEM supplemented with 10% fetal calf serum. During the next 2 days, embryos that attached and formed trophoblastic outgrowths were scraped off the dish and the *agouti* locus genotype of each embryo was determined using a PCR-based assay as previously described (Frohman *et al.*, 1993). The assay determines inheritance of a variant *Hin*dIII site, present on the a^x allele and absent from the *a* allele, located ≤1 cM distal to the *agouti* locus (Lovett *et al.*, 1987; Siracusa *et al.*, 1989; Miller *et al.*, 1993).

To determine whether inhibition of SAHase affected development of non-mutant embryos, blastocysts obtained from superovulated FVB/N mice were placed into *in vitro* microdrop culture with DMEM supplemented with 10% fetal calf serum (control), or the same medium to which 3′-deaza-aristeromycin had been added to a final concentration of 0.5, 2.0, 10 or 20 μM. Photographs of the embryos taken every day for a 4 day period were used to assign a phenotypic score for each embryo as follows: category 0, intact or partially intact zona pellucida; category 1, complete 'hatching' from the zona pellucida without attachment to the substrate; category 2, attachment of trophectoderm with little or no inner cell mass evident; category 3, limited proliferation of the inner cell mass and category 4, extensive differentiation of the inner cell mass.

To determine whether increased intracellular concentrations of adenosine would inhibit development of non-mutant embryos, we made use of the ability to reverse the SAHase reaction by increasing the concentration of intracellular adenosine (Kredich and Hershfield, 1989). Blastocysts obtained as described above were cultured in medium which contained 50 μM uridine (control), or the same medium supplemented with adenosine (Ado), 2′-deoxycoformycin (dCF) or Ado + dCF. Ado and dCF were used at final concentrations of 50 μM and 2 μM, respectively. The uridine was added to prevent the depletion of cellular pyrimidine nucleotides that has been observed in some cultured cells as a secondary effect of adenosine (Green and Chan, 1973; Hershfield *et al.*, 1977). Embryos were photographed and scored as described above.

Acknowledgements

We thank Virginia Papaioannou for providing animals carrying the a^x allele, and Kimberly Miller, Elaine Carlson and Stephane Toutain for technical assistance. This work was supported in part by HG-00377 (G.S.B.), by HD-03132 (C.J.E.) and by DK-20902 (M.S.H.) from the National Institutes of Health. G.S.B. is an Assistant Investigator of the Howard Hughes Medical Institute.

References

Andria,M.L., Barsh,G.S. and Levy,S. (1982) *Biochem. Biophys. Res. Commun.*, **186**, 1201–1206.

Arredondo-Vega,F.X., Kurtzberg,J., Chaffee,S., Santisteban,I., Reisner,E., Povey,M.S. and Hershfield,M.S. (1990) *J. Clin. Invest.*, **86**, 444–452.

Barsh,G.S. and Epstein,C.J. (1989a) *Genomics*, **5**, 9–18.

Barsh,G.S. and Epstein,C.J. (1989b) *Genetics*, **121**, 811–818.

Borchardt,R.T., Usdin,E. and Creveling,C.R. (1982) *Biochemistry of S-adenosylmethionine and Related Compounds*. Macmillan, London.

Bultman,S.J., Michaud,E.J. and Woychik,R.P. (1992) *Cell*, **71**, 1195–1204.

Chiang,P.K., Burbelo,P.D., Brugh,S.A., Gordon,R.K., Fukuda,K. and Yamada,Y. (1992) *J. Biol. Chem.*, **267**, 4988–4991.

Cizadlo,G.R. and Granholm,N.H. (1978) *Genetica*, **48**, 89–93.

Cools,M. and De Clercq,E. (1990) *Biochem. Pharmacol.*, **40**, 2259–2264.

Costantini,F., Radice,G., Lee,J.L., Chada,K.K., Perry,W. and Son,H.J. (1989) *Prog. Nucleic Acids Res. Mol. Biol.*, **36**, 159–169.

Coulter-Karis,D.E. and Hershfield,M.S. (1989) *Ann. Hum. Genet.*, **53**, 169–175.

Cuènot,L. (1908) *Arch. Zool. Exper. Gener.*, **9**, 7–15.

De La Haba,G. and Cantoni,G. (1959) *J. Biol. Chem.*, **234**, 603.

Duerre,J.A., Buttz,H.R. and Ackerman,J.J. (1992) *Biochem. Cell Biol.*, **70**, 703–711.

Eaton,G.J. and Green,M.M. (1962) *Genetica*, **33**, 106–112.

Friedrich,G. and Soriano,P. (1991) *Genes Dev.*, **5**, 1513–1523.

Frohman,M.A., Martin,G.R., Cordes,S.P., Halamek,L.P. and Barsh,G.S. (1993) *Development*, **117**, 925–936.
Galbraith,D.B., Wolff,G.L. and Brewer,N.L. (1979) *Dev. Genet.*, **1**, 167–179.
Green,H. and Chan,T. (1973) *Science*, **182**, 836–837.
Green,M.C. (1989) *Catalogue of Mutant Genes and Polymorphic Loci*. 2nd edn. Oxford University Press, UK.
Greenberg,M.L., Chaffee,S. and Hershfield,M.S. (1989) *J. Biol. Chem.*, **264**, 795–803.
Henderson,D.M., Hanson,S., Allen,T., Wilson,K., Coulter,K.D., Greenberg,M.L., Hershfield,M.S. and Ullman,B. (1992) *Mol. Biochem. Parasitol.*, **53**, 169–183.
Herrmann,B.G., Labeit,S., Poustka,A., King,T.R. and Lehrach,H. (1990) *Nature*, **343**, 617–622.
Hershfield,M.S. (1979) *J. Biol. Chem.*, **254**, 22–25.
Hershfield,M.S. and Francke,U. (1982) *Science*, **216**, 739–742.
Hershfield,M.S., Aiyar,V.N., Premakumar,R. and Small,W.C. (1985) *Biochem. J.*, **230**, 43–52.
Hershfield,M.S., Snyder,F.F. and Seegmiller,J.E. (1977) *Science*, **197**, 1284–1287.
Herz,J., Clouthier,D.E. and Hammer,R.E. (1992) *Cell*, **71**, 411–421.
Jaenisch,R. and Jahner,D. (1984) *Biochim. Biophys. Acta*, **782**, 1–9.
Kasir,J., Aksamit,R.R., Backlund,P.J. and Cantoni,G.L. (1988) *Biochem. Biophys. Res. Commun.*, **153**, 359–364.
Kredich,N.M. and Hershfield,M.S. (1979) *Proc. Natl Acad. Sci. USA*, **76**, 2450–2454.
Kredich,N.M. and Hershfield,M.S. (1980) *Adv. Enzyme Regul.*, **18**, 181–191.
Kredich,N.M. and Hershfield,M.S. (1989) In Scriver,C.R., Beaudet,A.L., Sly,W.S. and Valle,D. (eds), *The Metabolic Basis of Inherited Disease*. McGraw-Hill, New York, pp. 1045–1076.
Kredich,N.M. and Martin,D.J. (1977) *Cell*, **12**, 931–938.
Lee,J.J., Radice,G., Perkins,C.P. and Costantini,F. (1992) *Development*, **115**, 277–288.
Lovett,M., Cheng,Z.Y., Lamela,E.M., Yokoi,T. and Epstein,C.J. (1987) *Genetics*, **115**, 747–754.
Lowry,O.H., Rosebrough,M.J., Farr,A.J. and Randall,A.J. (1951) *J. Biol. Chem.*, **193**, 265–275.
Lyon,M.F., Fisher,G. and Glenister,P.H. (1985) *Genet. Res.*, **46**, 95–99.
Magnuson,T. (1986) In Rossant,J. and Pedersen,R.A. (eds), *Experimental Approaches to Mammalian Embryonic Development*. Cambridge University Press, UK, pp. 437–474.
Michaud,E.J., Bultman,S.J., Stubbs,L.J. and Woychik,R.P. (1993) *Genes Dev.*, **7**, 1203–1213.
Miller,M.W., Duhl,D.M.J., Vrieling,H., Cordes,S.P., Ollmann,M.M., Winkes,B.M. and Barsh,G.S. (1993) *Genes Dev.*, **7**, 454–467.
Mohandas,T., Sparkes,R.S., Suh,E.J. and Hershfield,M.S. (1984) *Hum. Genet.*, **66**, 292–295.
Niswander,L., Yee,D., Rinchik,E.M., Russell,L.B. and Magnuson,T. (1989) *Development*, **105**, 175–182.
Ogawa,H., Gomi,T., Mueckler,M.M., Fujioka,M., Backlund,P.J., Aksamit,R.R., Unson,C.G. and Cantoni,G.L. (1987) *Proc. Natl Acad. Sci. USA*, **84**, 719–723.
Papioannou,V.E. and Mardon,H. (1983) *Dev. Genet.*, **4**, 21–29.
Pedersen,R.A. (1974) *J. Exp. Zool.*, **188**, 307–320.
Pilz,A., Le,T.P., Moseley,H., Peters,J. and Abbott,C. (1992) *Mammalian Genome*, **3**, 633–636.
Prasad,S.S., Starr,T.V. and Rose,A.M. (1993) *Genome*, **36**, 57–65.
Rinchik,E.M., Russell,L.B., Copeland,N.G. and Jenkins,N.A. (1986) *Genetics*, **112**, 321–342.
Rinchik,E.M., Stoye,J.P., Frankel,W.N., Coffin,J., Kwon,B.S. and Russell,L.B. (1993) *Mutat. Res.*, **286**, 199–207.
Robertson,G.G. (1942) *J. Exp. Zool.*, **89**, 197–231.
Rosssant,J. and Papaioannou,V.E. (1984) *Cell Differ.*, **15**, 155–161.
Russell,L.B., McDaniel,M.N.C. and Woodiel,F.N. (1963) *Genetics*, **48**, 907.
Russell,W.L. (1951) *Cold Spring Harbor Symp. Quant. Biol.*, **16**, 327–336.
Salvatore,F., Borek,E., Sappia,V., Williams-Ashman,H.G. and Schlenk,F. (1977) *The Biochemistry of S-adenosylmethionine*. Columbia University Press, New York.
Schnieke,A., Harbers,K. and Jaenisch,R. (1983) *Nature*, **304**, 315–320.
Silvers,W.K. (ed.) (1979) *The Coat Colors of Mice*. Springer-Verlag, New York, pp. 6–44.
Siracusa,L.D. (1991) *Ann. NY Acad. Sci.*, **642**, 419–430.
Siracusa,L.D. and Abbott,C.M. (1992) *Mammalian Genome*, **3**, S20–S24.
Siracusa,L.D., Russell,L.B., Eicher,E.M., Corrow,D.J., Copeland,N.G. and Jenkins,N.A. (1987) *Genetics*, **117**, 93–100.
Siracusa,L.D., Buchberg,A.M., Copeland,N.G. and Jenkins,N.A. (1989) *Genetics*, **122**, 669–679.
Snow,M.H. and Bennett,D. (1978) *J. Embryol. Exp. Morphol.*, **47**, 39–52.
Vrieling,H., Duhl,D.M.J., Millar,S.E., Miller,K.A. and Barsh,G.S. (1994) *Proc. Natl Acad. Sci. USA*, in press.
Walker,R.D. and Duerre,J.A. (1975) *Can. J. Biochem.*, **53**, 312–319.
Wallace,M.E. (1965) *J. Hered.*, **56**, 267–271.
West,J.D., Flockhart,J.H., Peters,J. and Ball,S.T. (1990) *Genet Res.*, **56**, 223–236.
Winkes,B.M., Ollmann,M.M. and Barsh,G.S. (1994) *Mammalian Genome*, **5**, 3–10.
Wolff,G.L., Roberts,D.W. and Galbraith,D.B. (1986) *J. Hered.*, **77**, 151–158.
Yen,T.T., Gill,A.M., Frigeri,L.G., Barsh,G.S. and Wolff,G.L. (1994) *FASEB J.*, in press.

Received on August 13, 1993; revised on January 14, 1994